*Anal. Bioanal. Electrochem., Vol. 11, No. 8, 2019, 1020-1031*

***Analytical & Bioanalytical Electrochemistry***



*Full Paper*

# Corrosion Behavior of PEO Coatings on 6061 Al Alloy: Effect of Sodium Fluoride Addition to Aluminate based Electrolyte

**Zahra Masoomi Loghman, Arash Fattah-alhosseini* and Seyed Omid Gashti**

*Department of Materials Engineering, Bu-Ali Sina University, Hamedan 65178-38695, Iran*

*Corresponding Author, Tel.: +988138292505; Fax: +988138257400

E-Mail: a.fattah@basu.ac.ir

*Received: 26 January 2019 / Received in revised form: 15 July 2019 / Accepted: 17 July 2019 / Published online: 31 August 2019*

**Abstract**- The present work has studied the effect of sodium fluoride on properties of plasma electrolytic oxidation (PEO) coatings. PEO coatings were formed on 6061 Al alloy in aluminate based electrolytes with different sodium fluoride concentrations. The results indicated that addition of sodium fluoride to the electrolyte prepared ceramic coating with high quality and therefore improved the corrosion resistance in 3.5 wt% NaCl solution. Scanning electron microscopy (SEM) images were used to examine the cross sectional and surface morphology of the coatings. The corrosion behavior of the PEO coatings were evaluated using electrochemical impedance spectroscopy (EIS). The corrosion behavior of the coatings improved by adding 1 g/L sodium fluoride into the electrolyte, but the corrosion resistance of the coatings decreased while adding more than 1 g/L sodium fluoride in electrolyte solution. The prepared sample in the electrolyte with 1 g/L sodium fluoride showed the best morphology with the least porosity and more corrosion resistance compared with other coatings.

**Keywords-** Sodium aluminate, Sodium fluoride, 6061 aluminum alloy, Plasma electrolytic oxidation

## 1. INTRODUCTION

Aluminum and its alloys have good corrosion resistance in most natural environments because of the passive oxide layer which is formed on their surfaces. However, corrosive

environments and the presence of alloying elements in aluminum make it susceptible to localized corrosion and led to destruction of the passive layer [1-5]. Various surface treatment techniques such as ion implantation, laser processing and anodic oxidation have been used for improving corrosion and wear resistance of aluminum. These methods were limited in industry due to the complexity of the process, high energy consumption and low thickness [6].

PEO is a novel surface modification to make a ceramic coating on the surface of the light metal alloys such as Mg, Ti, Al, Ta, Nb and their alloys [7]. PEO coatings are extensively used for aerospace, biomedical devices, textile industry, automotive engineering and other industrials production [8]. This method has many advantages such as low cost, simple process technique and low environmental damaging compared to other traditional methods. PEO coatings improve corrosion and wear resistance of metals. Coatings with a thickness of 200 mm can be created by the PEO process, whereas micrometer thick coatings can also protect the base metal. Therefore thick coatings with high energy consumption decreased efficiency of the PEO process [6].

Unique properties of PEO coating is required for different applications. The morphology and microstructure of the PEO coating can be changed by controlling the process [9]. The PEO process is a progressive anodic oxidation that oxide ceramic layers are produced by a plasma discharge electrolyte [10]. In the PEO process, there is strong adhesion between a metal substrate and a ceramic coating [11]. The temperature of substrate is kept low during the PEO process so there is no effect of heat on the metallic substrate [12].

In the PEO coating process the samples were coated in an aqueous solution. High applied potential during PEO process led to the formation of micro discharges. Micro discharges are the crucial characteristic of PEO process [13]. The properties of short-lived micro discharges have an important effect on composition, morphology and structure of the coating [14]. During the subsequent anodic pulse the holes which formed in the cathodic breakdown will be repaired. Hence, despite the high porosity, the PEO coatings layers preserve the substrate effectively against the corrosion [15]. In the PEO process, different organic compounds can be added to the electrolyte to modify the electrolyte and formed coatings with good properties such as wear and corrosion resistance [16].

Hsu et al. [17] examined the addition effects of $Al(NO_3)_3$ to the $NaAlO_2$ electrolyte and concluded $Al(NO_3)_3$ effects on voltage-time response of process. Appropriate addition amount of $Al(NO_3)_3$ to the coating solution, increased the $\alpha$-$Al_2O_3$ content in the coating and improved the hardness of the coating significantly. Kaseem et al. [16] investigated the effect of sodium benzoate in an alkaline aluminate solution on the corrosion resistance of 6061 Al alloy coated by PEO and concluded that the presence of sodium benzoate in the coating, enhanced corrosion behavior of the coating. Yeh et al. [18] examined influence of urea and sodium nitrite in aluminate based electrolyte on properties of PEO coating on 6061 aluminum alloy. They concluded these two additives have different effects on film growth. Addition of urea in

electrolyte improved the content of nitrogen in PEO layer and reduces the thickness and increases the porosity of the coating, while sodium nitrite increases the layer thickness and diminishes porosity of the PEO coating.

In recent years, effect of different additives to PEO coatings on 6061 aluminum alloy has been investigated, but effect of sodium fluoride on properties of PEO coatings on 6061 Al alloys has not been studied. In the present paper, we studied the effect of sodium fluoride on properties of PEO coatings on 6061 Al alloy. The PEO coatings were produced without and with different concentrations of sodium fluoride in aluminate based solution. The microstructure and micro-pores in the different coatings were studied. The corrosion resistance of the PEO coatings in 3.5 wt% NaCl solution were also evaluated.

## 2. EXPERIMENTAL PROCEDURES

Samples of 6061 aluminum alloy with dimensions 2 cm×2 cm×0.2 cm, were polished and washed by ethanol under ultrasonic. After that, the samples were dried by cold air and placed in the electrolyte as the anode and the stainless steel container was used as a cathode. The solution temperature was controlled at 30 ˚C by a cooling system. The electrolyte contains a combination of 10 g/L sodium aluminate, 1 g/L sodium hydroxide and 0-3 g/L sodium fluoride. The samples code was indicated in Table 1. The conductivity of the solutions measured using D812 Weilheim instrument.

**Table1**. Composition and pH value of electrolytes used for PEO process of 6061 aluminum alloy

| Sample code | $NaAlO_2$ (g/L) | NaOH (g/L) | NaF (g/L) | pH |
|---|---|---|---|---|
| S1 | 10 | 1 | 0 | **12.4** |
| S2 | 10 | 1 | 1 | **12.6** |
| S3 | 10 | 1 | 2 | **12.7** |
| S4 | 10 | 1 | 3 | **12.9** |

The process carried out using DC current mode at constant current density of 15 A/dm$^2$ for 900 s. The surface morphology and the cross section of coated samples were observed by JEOL JSM-840A SEM and thickness of the coatings measured by cross sectional image using the Digimiser software. Phase composition evaluated by the Italstructures APD2000 diffractometer in the 2θ range of 20˚ to 90˚ with 0.05° step size using Cu Kα radiation. The conventional 3-electrode cell including Pt plate as the counter electrode and Ag/AgCl saturated in KCl as the reference electrode were used for evaluating the corrosion of coating. The NOVA 1.11 software was used for modeling the EIS data and fitting curves. The electrochemical

measurements were obtained by μAutolab Type III/FRA2 system. The EIS tests were implemented at open-circuit potential (OCP) condition and AC potential with the amplitude of 10 mV and a frequency range of 100 kHz to 10 mHz. The working electrodes plunged in 3.5 wt% NaCl solution for 7200 s. All measurements were repeated at least three times.

## 3. RESULTS AND DISCUSSION

### 3.1. Voltage-time behavior

Applying the constant current mode, various voltages were monitored in PEO process. The voltage-time curve shows the voltage variation as a function of coating time [17,19]. Fig. 1 illustrates the voltage-time plot of the coatings formed in different concentrations of sodium fluoride in constant current density of 15 A/dm$^2$. Three stages can be seen in the voltage-time response of the PEO process. In stage (1), voltage increases linearly with time. In stage (2), the slope of voltage-time curve decreases and sparks appear on the surface of sample. This voltage is known as a breakdown voltage. Stage (3) is a crucial stage of PEO process and the coating is formed in this stage. In this stage, voltage-time slope is constant and the sparking is monotonous [20].

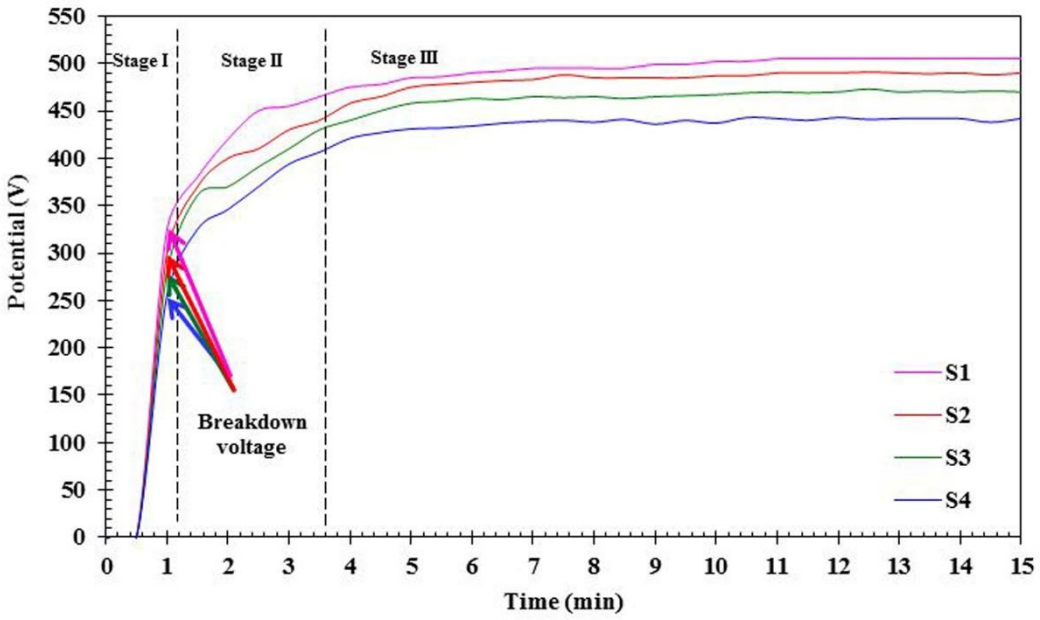


**Fig. 1.** Potential-time response of PEO coatings on 6061 aluminum alloy in different concentration of sodium fluoride in electrolytes

The voltage-time plot revealed that breakdown voltage decreased as the sodium fluoride concentration increased in the electrolyte. The fluorine anions increased the conductivity [21]. In the other words by adding sodium fluoride to the solution, the conductivity increases and leads to rapid initiation of sparking phenomena. As illustrated in Fig. 1, the maximum voltage

of solutions increased by adding sodium fluoride. Hence, adding sodium fluoride into the electrolyte solution increases the conductivity and decreases the breakdown voltage of the electrolyte. Variation of conductivity and breakdown voltage of the coatings solutions with addition of sodium fluoride in the electrolyte were showed in Fig. 2. As presented in Fig. 2, the electrolyte without sodium fluoride had the lowest conductivity and with addition of sodium fluoride to the electrolyte, conductivities value increased. So the electrolyte containing 3 g/L sodium fluoride had the lowest sparking and maximum voltage during the PEO process. The highest sparking and maximum voltage were observed for the electrolyte without sodium fluoride [22].

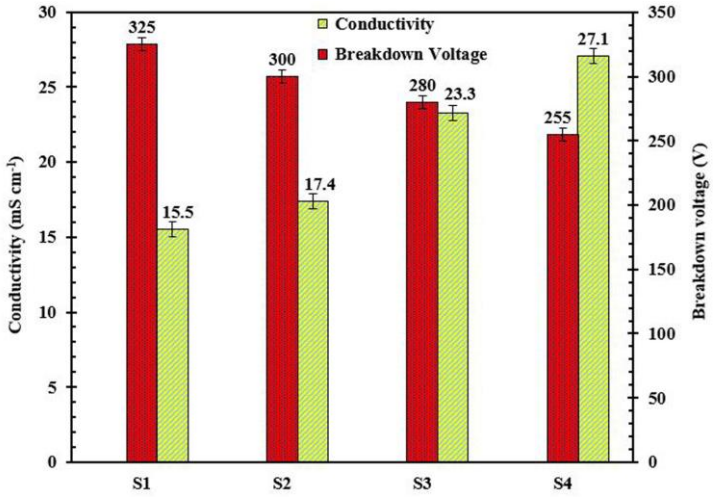


**Fig. 2.** Variation of conductivity and breakdown potential *vs*. concentration of sodium fluoride in electrolytes

### 3.2. Surface morphology and thickness of the coatings

Micro-pores on the surface of PEO coatings originated from micro-discharging are the characteristics of ceramic coatings [23]. Typically three layers exist in PEO coatings, an outer porous layer, an inner compact layer and a transition layer [24]. The surface and cross sectional morphologies of the PEO coatings prepared in different concentration of sodium fluoride in different magnifications were showed in Fig. 3a, c, e, g. The electrolyte containing fluoride improves the quality of the coating [25]. Coatings containing sodium fluoride have less porosity and roughness on the coatings surface compared with the coating without sodium fluoride. Distribution of $Al^{3+}$ ions between the micro-holes which is the effect of $F^-$ ions transudation into the coating under electric field force leads to a reduction in surface porosity and roughness [26]. Fig. 3a illustrates the surface morphology of the coating prepared in 10 g/L sodium aluminate and 1 g/L sodium hydroxide. The island-like structure with feature of porosity can be seen in the surface of the coating. By addition of 1 g/L sodium fluoride to electrolyte, the sparking density became homogeneous and surface became smoother and the structure of the coating changed to pancake-like structure with feature of low porosity [26,27].

As the concentration of sodium fluoride increased to 2 and 3 g/L, the feature of surface declined and porosities formed in the structure. Powerful sparking at the end of PEO process produced these porosities on the surface of the coatings formed in solutions with 2 and 3 g/L sodium fluoride [27,28]. The electrolyte composition significantly affected the size of micro-pores [29].

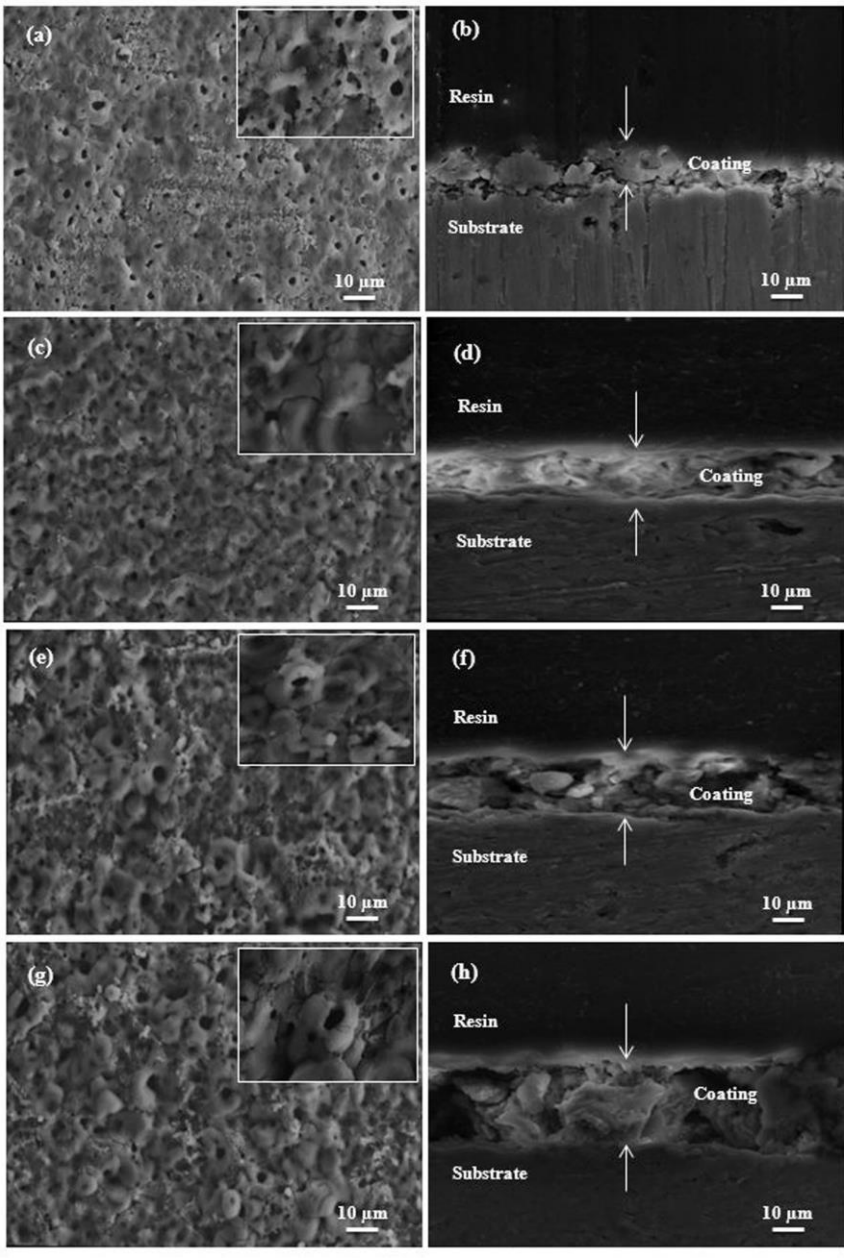


**Fig. 3.** SEM images of the plan view and cross-section view of 6061 aluminum alloy with PEO coatings: (a) and (b) S1; (c) and (d) S2; (e) and (f) S3; (g) and (h) S4 samples

The average size of micro-pores on the surface of the coatings in different concentrations of sodium fluoride is indicated in Fig. 4. The average size of pores in the coating with 1 g/L

sodium fluoride is lower than other coatings. Strong sparking with addition of 2 and 3 g/L sodium fluoride in electrolyte led to formation of large pores in the coatings but the number of discharge channel is lower than coating without sodium fluoride [21,30]. The coating was formed without sodium fluoride contains numerous small pores. However, adding sodium fluoride led to fewer and larger pores in the coatings [31]. Some micro-cracks can be seen in the surface of the coatings. Generated thermal stresses from rapid solidification of molten oxides made some micro-cracks on the surface of the coatings because of contacting with cold electrolyte [32]. The high plasma temperature on the surface of aluminum alloy led to formation of melting product around the volcano pores [28].

The cross-sectional morphologies of different coatings presented in Fig. 3b, d, f, h. The thickness of the PEO coating increases with addition of fluoride ion to the electrolyte [26,31]. The growth of PEO coatings is increased by adding sodium fluoride in electrolyte and increases the thickness of coatings [27]. The cross-sectional image of coating prepared without sodium fluoride showed a porous and thin layer but the coating with 1 g/L sodium fluoride in its electrolyte showed a compact and uniform layer. With increasing sodium fluoride concentration in the electrolyte, the cross-sectional morphology of coating showed layer containing porosities. The powerful sparking makes a porous structure with increasing the sodium fluoride content in the electrolyte [30]. The thickness of the coatings which is formed in different concentration of sodium fluoride is presented in Fig. 5. Accordingly, increasing sodium fluoride concentration in the electrolyte caused the coating to become thicker.

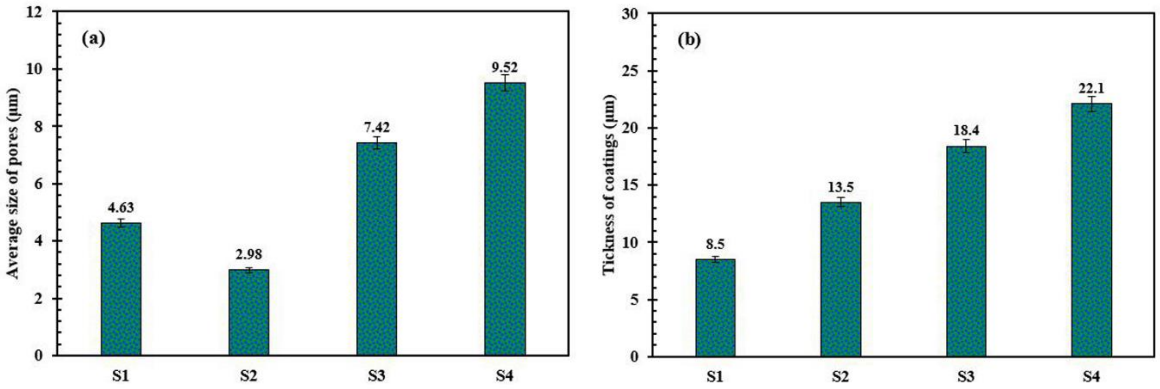


**Fig. 4.** (a) Average size of pores and (b) thickness of PEO coatings prepared in different concentration of sodium fluoride in the electrolyte

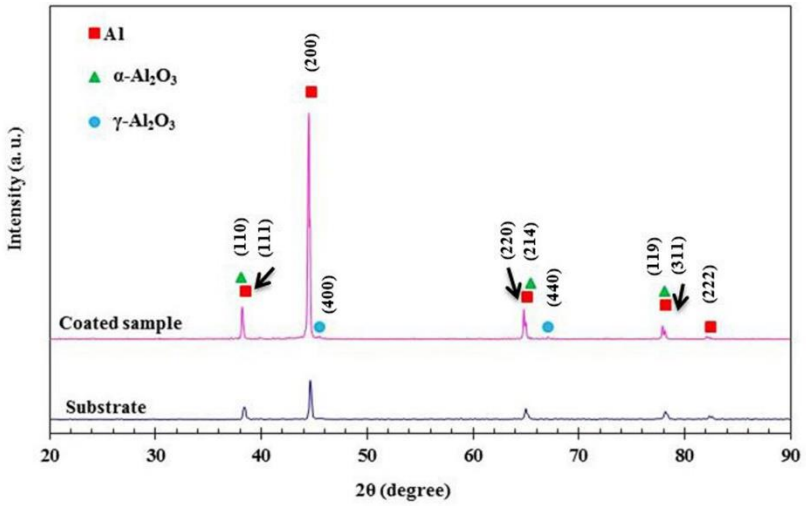


**Fig. 5.** X-ray diffraction pattern of 6061 aluminum alloy with and without PEO coating

### 3.3. Composition of the coatings

In the PEO coating process of aluminum, hard and thick $Al_2O_3$ layer is formed on an aluminum substrate [11]. The composition of the PEO coating on aluminum alloy includes composition of the mainly α-$Al_2O_3$ and γ-$Al_2O_3$. Electrolyte changes can alter the composition of the coating [33]. At the beginning of PEO process γ-$Al_2O_3$ phase formed due to the low thickness of coating at the early stage of PEO process, γ-$Al_2O_3$ transformation to hard α-$Al_2O_3$ does not occur. Increasing the temperature in other stages of coating process γ-$Al_2O_3$ transforms to α-$Al_2O_3$ which is stable phase [16, 34-36]. The thickness of the coating increased in the later stage of process and γ-$Al_2O_3$ to α-$Al_2O_3$ transition occurs [35].

The XRD diffraction pattern of aluminate based coating containing 1 g/L sodium fluoride is illustrated in Fig. 6. The phases that can be seen in the analysis mainly contain α-$Al_2O_3$ and γ-$Al_2O_3$. The strong aluminum peaks were seen in the XRD pattern of the coating. Presence of aluminum peaks in the XRD pattern of the coating is explained by two reasons: (1) Low thickness of the coating compared with the depth of X-ray radiation and (2) The presence of micro-pores on the surface of the coating to penetrate the X-ray into the substrate [37]. The observed aluminum peaks in the analysis of the coating should be ignored because they are related to aluminum substrate [38]. No fluorine-containing crystalline phases were observed in the XRD pattern [31].

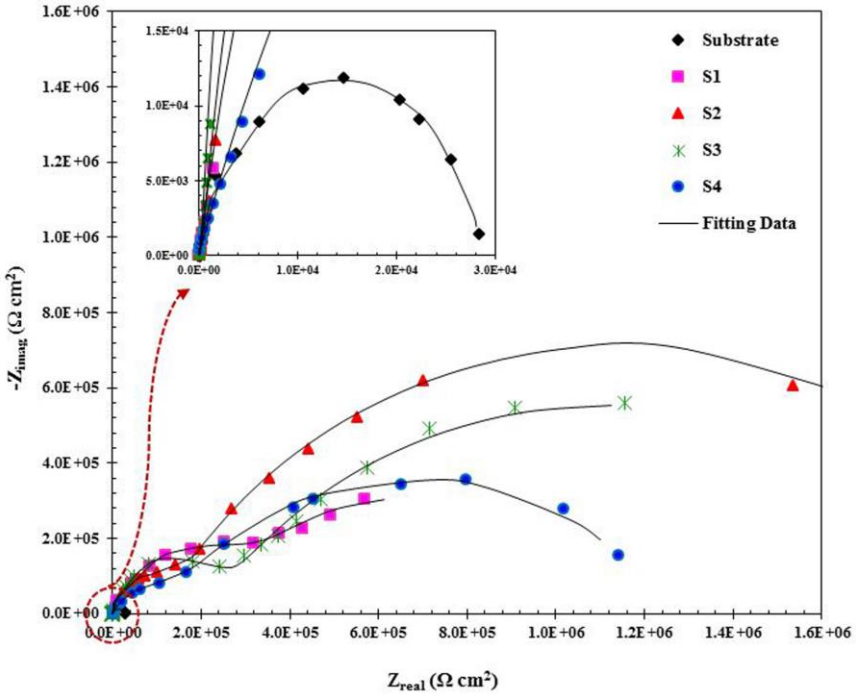


**Fig. 6.** Nyquist plots of PEO coatings on 6061 aluminum alloy in different concentration of sodium fluoride in electrolytes

### 3.4. Corrosion behavior

The obtained Nyquist plots for PEO coatings and substrate in 3.5 wt % NaCl solution is presented in Fig. 6. The EIS plot for substrate at all frequency regions contains one capacitive semicircle representing a single time constant while the EIS spectra for PEO coatings contains two capacitive semicircle representing two time constants.

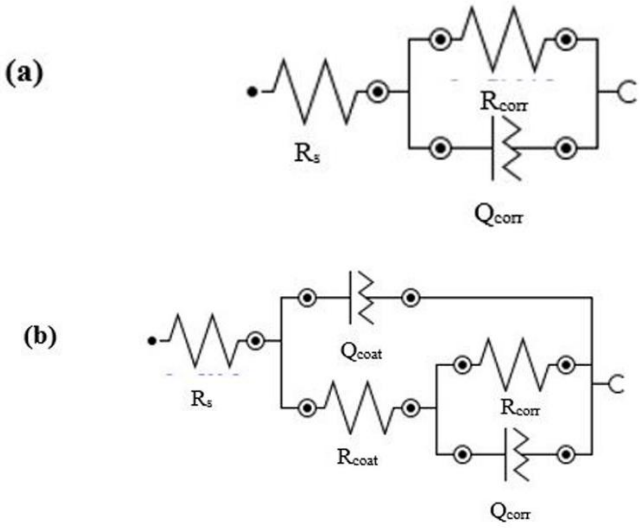


**Fig. 7.** Equivalent circuit model used to fit the experimental EIS data of (a) substrate, and (b) PEO coating samples

**Table 2.** Extracted data from electrical equivalent circuits of all Nyquist plots

| Sample | $R_{sol}$ ($\Omega cm^2$) | $R_{coat}$ ($\Omega cm^2$) | $R_{corr}$ ($\Omega cm^2$) |
|---|---|---|---|
| **Substrate** | 56 | - | $71.3\times10^3$ |
| **S1** | 56 | $842\times10^3$ | $1.7\times10^6$ |
| **S2** | 54 | $305\times10^3$ | $5.21\times10^6$ |
| **S3** | 55 | $568\times10^3$ | $4.46\times10^6$ |
| **S4** | 52 | $356\times10^3$ | $2.76\times10^6$ |

The smaller semicircle is related to coating layer and the bigger semicircle is related to electrical double layer of the metal surface. The electrical equivalent circuit model used to fit the Nyquist plots of (a) substrate, and (b) PEO coating samples are shown in Fig. 7. In circuit (a), $R_s$ is the solution resistance, $R_{corr}$ is corrosion resistance and $Q_{corr}$ is constant phase element (CPE). In circuit (b), $R_{coat}$ is related to corrosion resistance and $Q_{coat}$ is CPE of coating layer [16]. The extracted resistance values of Nyquist plots of the coated samples and 6061 aluminum alloy are shown in Table 2. Based on the extracted values, it can be seen that the corrosion resistance of coated sample increased while adding sodium fluoride to electrolyte. On the other hand, by increasing sodium fluoride concentration from 1 g/L to 3 g/L this parameter decreased. The main reason of this phenomena is related to the thickness and pores size values of coating that reported in Fig. 4. Increasing sodium fluoride concentration made the thickness of coatings increase in addition to their pores size. So, by increasing pores size, corrosion was accelerated and the corrosion resistance of sample decreased. Therefore, the electrolyte containing 1 g/L sodium fluoride has the best value of corrosion resistance ($5.21\times10^6\ \Omega\ cm^2$) that is 73 times more than corrosion resistance of the uncoated sample. In addition, among the coated samples, this value is greater than others that related to lower average pores size (2.98 μm) of it.

## 4. CONCLUSION

The influence of different concentration of sodium fluoride in the electrolyte on corrosion behavior and microstructure of the PEO coatings on 6061 Al alloy is investigated in this work. The surface morphology of the coatings was improved by addition of sodium fluoride in the electrolyte. The additions of sodium fluoride increases the pore size while diminishes the number of pores in the coatings. The coatings containing sodium fluoride in the electrolyte presented lower porosity in the surface. The thickness of the coating increased by adding

sodium fluoride in the electrolyte and increased its concentration. The thickness of the coating with 3 g/L sodium fluoride in the electrolyte is about 22.1 μm. However, increasing sodium fluoride concentration made the pores of coating increase. The electrolyte containing 1 g/L sodium fluoride has the optimum value of thickness and pores size. The coated samples in the electrolyte with sodium fluoride showed superior corrosion resistance compared with the coating formed in the electrolyte without sodium fluoride. In the solution containing 1 g/L sodium fluoride, the corrosion resistance increased about 73 times compared to the electrolyte without sodium fluoride. On the other hand, by increasing sodium fluoride concentration, the corrosion resistance decreased.

## REFERENCES

[1] B. Zaid, N. Maddache, D. Saidi, N. Souami, N. Bacha, and A. Si Ahmed, J. Alloys Compd. 629 (2015) 188.
[2] S. O. Gashti, and A. Fattah-alhosseini, Anal. Bioanal. Electrochem. 6 (2014) 535.
[3] A. Fattah-alhosseini, S. O. Gashti, and M. Molaie, J. Mater. Eng. Perform. 27 (2018) 825.
[4] M. Vakili-Azghandi, A. Fattah-alhosseini, and M. K. Keshavarz, Measurement 124 (2018) 252.
[5] M. Vakili-Azghandi, A. Fattah-alhosseini, and M. K. Keshavarz, J. Mater. Eng. Perform. 25 (2016) 5302.
[6] K. Dejun, L. Hao, and W. Jinchun, J. Alloys Compd. 650 (2015) 393.
[7] Q. Tran, Y. Kuo, J. Sun, J. He, and T. Chin, Surf. Coat. Technol. 303 (2016) 61.
[8] A. Khodabandeloie, and A. Fattah-alhosseini, Anal. Bioanal. Electrochem. 10 (2018) 1574.
[9] V. Dehnavi, B. Li Luan, X. Yang Liu, D. W. Shoesmith, and S. Rohani, Surf. Coat. Technol. 269 (2015) 91.
[10] R. H. U. Khan, A. Yerokhin, X. Li, H. Dong, and A. Matthews, Surf. Coat. Technol. 205 (2010) 1679.
[11] R. Chaharmahali, M. Shadabi, K. Babaei, S. O. Gashti, and A. Fattah-alhosseini, Anal. Bioanal. Electrochem. 11 (2019) 38.
[12] L. Wen, Y. Wang, Y. Jin, B. Liu, Y. Zhou, and D. Sun, Surf. Coat. Technol. 228 (2013) 92.
[13] R. Chaharmahali, K. Babaei, and A. Fattah-alhosseini, Anal. Bioanal. Electrochem. 11 (2019) 703.
[14] V. Dehnavi, D. W. Shoesmith, B. Luan, M. Yari, X. Liu, and S. Rohani, Mater. Chem. Phys. 161 (2015) 49.
[15] A. Lugovskoy, M. Zinigrad, A. Kossenko, and B. Kazanski, Appl. Surf. Sci. 264 (2013) 743.

[16] Z. Masoomi Loghman, A. Fattah-alhosseini, and S. O. Gashti, Anal. Bioanal. Electrochem. 10 (2018) 1247.
[17] C. Hsu, H. Teng, and F. Lu, Surf. Coat. Technol. 205 (2011) 3677.
[18] S. Yeh, D. Tsai, Sh. Guan, and Ch. Chou, Appl. Surf. Sci. 356 (2015) 135.
[19] A. Fattah-Alhosseini, M. Vakili-Azghandi, and M. K. Keshavarz, Acta Metall. Sin. Engl. 29 (2016) 274.
[20] S. Sarbishei, M. Faghihi Sani, and M. Mohammadi, Vacuum 108 (2014) 12.
[21] A. Němcováa, P. Skeldon, G. E. Thompson, and B. Pacal, Surf. Coat. Technol. 232 (2013) 827.
[22] H. Guo, and M. An, Appl. Surf. Sci. 246 (2005) 229.
[23] Y. Yürektürk, F. Muhaffel, and M. Baydoan, Surf. Coat. Technol. 269 (2015) 83.
[24] J. H. Wang, M. H. Du, F. Z. Han, and J. Yang, Appl. Surf. Sci. 292 (2014) 658.
[25] A. Kossenko, and M. Zinigrad, Mater. Des. 88 (2015) 302.
[26] Zh. Wang, L. Wu, W. Cai, and Zh. Jiang, J. Alloys Compd. 505 (2010) 188.
[27] Y. Wang, Zh. Liu, J. Ouyang, Y. Wang, and Y. Zhou, Appl. Surf. Sci. 258 (2012) 8946.
[28] L. Wang, L. Chen, Z. Yan, H. Wang, and J. Peng, J. Alloys Compd. 480 (2009) 469.
[29] S. Lee, and D. Toan, Surf. Coat. Technol. 307 (2016) 781.
[30] H. Khanmohammadi, S. Allahkaram, N. Towhidi, and A. Rashidfarokhi, Surf. Eng. 32 (2016) 448.
[31] B. Kazanski, A. Kossenko, M. Zinigrad, and A. Lugovskoy, Appl. Surf. Sci. 287 (2013) 46.
[32] A. Fattah-alhosseini, and M. Sabaghi Joni, J. Mater. Eng. Perform. 24 (2015) 3444.
[33] Y. Guan, Y. Xia, and G. Li, Surf. Coat. Technol. 202 (2008) 4602.
[34] T. Wei, F. Yan, and J. Tian, J. Alloys Compd. 389 (2005) 169.
[35] Y. Oh, J. Mun, and J. Kim, Surf. Coat. Technol. 204 (2009) 141.
[36] M. Vakili-Azghandi, and A. Fattah-alhosseini, Metallurgical and Materials Transactions A 48 (2017) 4681.
[37] A. Bahramian, K. Raeissi, and A. Hakimizad. Appl. Surf. Sci. 351 (2015) 13.
[38] E. Erfanifar, M. Aliofkhazraei, H. FakhrNabavi, H. Sharifi, and A. Sabour-Rouhaghdam, Mater. Chem. Phys. 185 (2017) 162.